
Geochemical Fingerprinting and Magmatic Plumbing Systems

Christophe Y. Galerne and Else-Ragnhild Neumann

Abstract

Subvolcanic systems are characterized by complex combinations of intrusive units (dykes, sills, saucer-shaped sills, cone sheets, etc.) for which genetic relationships are unclear. This chapter explains how whole-rock geochemistry may be used to resolve the genetic relationships of such subvolcanic (and volcanic) systems. We start with a short introduction of the geochemical fingerprinting method with particular emphasis on the statistical refinement method called Forward Stepwise-Discriminant Function Analysis (FS-DFA). Combined with field mapping and structural analysis, geochemical fingerprinting based on major and trace elements and isotope ratios, is a very powerful tool to distinguish between igneous units (lavas, sills, dykes) with subtle (or not so subtle) geochemical differences. Different geochemical fingerprinting or signatures indicate derivation from distinct magma batches. The results from FS-DFA analyses may be used to reveal genetic relationships between geological units, or lack of such, which again may be used to throw light on subvolcanic plumbing systems, the feeding system in sill-dyke complexes, as well as other problems. The method is illustrated by studies of the Golden Valley Sill Complex in the Karoo Basin (South Africa).

1 Introduction

Comprehension of the processes that give rise to different types of units (dykes, sills, lavas) in magmatic domains (flood basalts, sill complexes in sedimentary basins, dyke-lava-sill relationships in volcanoes, etc.) depends strongly on information about the genetic relationships between different units. Important information may be obtained from field observations and geophysical imaging (e.g. seismic analyses). However, although the physical relationships

C.Y. Galerne (✉)
GeoModellingSolutions GmbH,
Hardturmstraße 120, 8005 Zurich, Switzerland
e-mail: christophe.y.galerne@googlemail.com

E.-R. Neumann
Physics of Geological Processes,
University of Oslo, Oslo, Norway
e-mail: e.r.neumann@geo.uio.no

between units may be identified by these methods, their genetic relationships are not ascertained. This is true for units that appear to be in direct physical contact, as well as for units that are not. An important additional method is to establish the geochemical signatures of the geological units in the area in question. Different geochemical signatures of two units imply derivation from different magma batches, whereas identical signatures imply derivation from the same, or chemically identical, magma batches. Further analysis of the geochemical signatures of the units in an area may be used to establish the evolutionary histories of the magmatic rocks (the causal mechanisms for observed compositional variations), and possible genetic relationships between the units.

This chapter gives a presentation of different methods for geochemical fingerprinting; the statistical method Forward Stepwise-Discriminant Function Analysis (FS-DFA) is described in some detail. The methods are illustrated by examples from the Karoo Large Igneous Province (South Africa), with emphasis on the results obtained in the Golden Valley Sill Complex (GVSC).

The chapter ends with a discussion of how geochemical fingerprinting may be used to throw light on feeding mechanisms between different units (sill-sill, dyke-lava, dyke-sill), and subsurface plumbing systems.

2 Chemical Fingerprinting

2.1 Element Ratios

Chemical fingerprinting was originally developed in order to map distinct lava flows in igneous provinces dissected by erosion and/or poorly exposed. The basic method is to use ratios between incompatible trace elements to identify different magmatic units (lavas, dykes, sills). The term “incompatible trace elements” is generally

used for elements that fit very poorly into the minerals in the mantle (where basaltic magmas are formed) and in minerals forming in a basaltic magma (e.g. Rb, Th, U, Nb, Ta, Zr, P, rare earth elements [REE], Zr, Ti, Y). In a magma, ratios between pairs of strongly and moderately incompatible or pairs of moderately and mildly incompatible trace elements will therefore not change during moderate degrees of fractional crystallization. This means that samples derived from the same magma reservoir will have similar ratios, whereas different batches generally will have different ratios. Other processes (contamination, assimilation, mixing between chemically distinct magmas, separation of a fluid phase, etc.), will generally modify ratios between incompatible trace elements.

Figures 1 and 2 show the use of geochemical fingerprinting on lavas in the Lesotho Lava Plateau (the Drakensberg Group) in the Karoo Basin (Marsh et al. 1997). Whole-rock analyses on lavas from numerous isolated sections (Fig. 1a) show slightly different ratios between pairs of incompatible elements, i.e. different geochemical fingerprints. These differences are expressed in ratio-ratio diagrams in Fig. 2. In ratio-ratio diagrams samples from the same unit are expected to plot in a tight cluster. Samples from different units may overlap in one diagram, but be separated in another, revealing different geochemical characteristics. By the help of several ratio-ratio diagrams it may be possible to distinguish the chemical identities of different magmatic units within the same area. Fig. 2 shows the results for lavas in the Lesotho Formation and in the Barkly East Formation in the Drakensberg Group. Lavas in the Barkly East formation form separate clusters in the two ratio-ratio diagrams, demonstrating different geochemical signatures. The chemical variations among the Lesotho lavas (Fig. 2), however, are too subtle to be differentiated in the ratio-ratio diagram and overlap in the grey field in Fig. 2. Based on ratio-ratio diagrams Marsh et al. (1997) were able to correlate lavas in

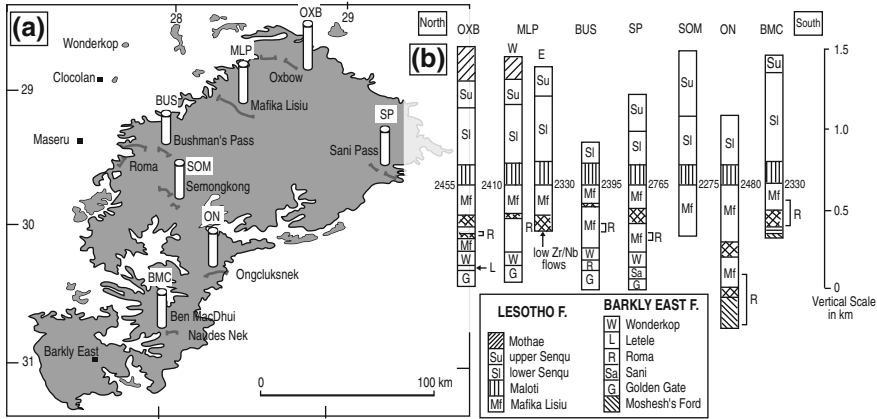


Fig. 1 Chemical fingerprinting of the Drakensberg lava sequence showing the correlation between the lava units at different localities. **a** Schematic map of the

Drakensberg flood basalts. **b** Summary of the stratigraphic columns in each location based on geochemistry after Marsh et al. (1997)

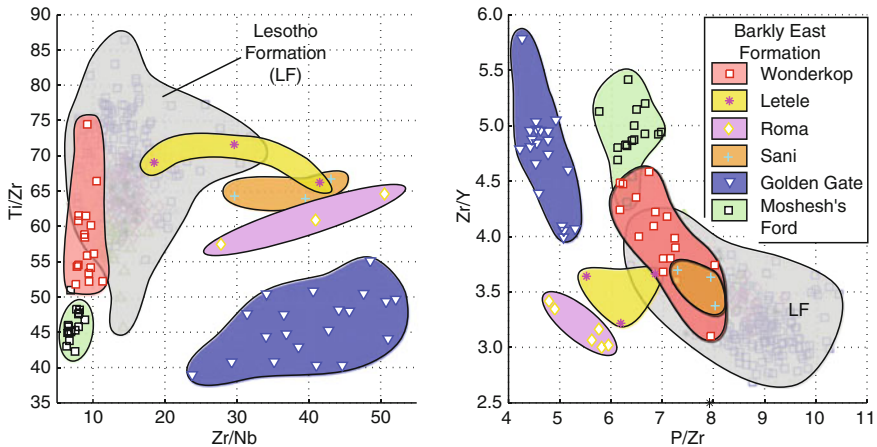


Fig. 2 Plots of ratio between strongly incompatible elements (Ti/Zr vs. Zr/Nb, Zr/Y vs. P/Zr) for lavas from the Lesotho Formation (*grey field*) and Barkly East

formation within the Drakensberg lava sequence (Marsh et al. 1997). See text for discussion

the Lesotho Formation and in the Barkly East Formation from one outcrop to the next (Fig. 1b). In this way they managed to map the extent of different lava flows, as well as time-related compositional variations.

Although ratios between highly incompatible elements are useful in revealing chemical contrasts in some cases, they clearly do not resolve subtle chemical contrasts. A more robust method is to use a statistical approach.

2.2 Statistical Methods

Statistical methods have proven to be excellent tools for distinguishing different geochemical signatures among magmatic rock units with small compositional contrasts (e.g. Duncan et al. 1984; Sheth et al. 2004). One such method is the Forward Stepwise-Discriminant Function Analysis (FS-DFA; Hill and Lewicki 2007; StatSoft 2013). Discriminant function analysis is a statistical

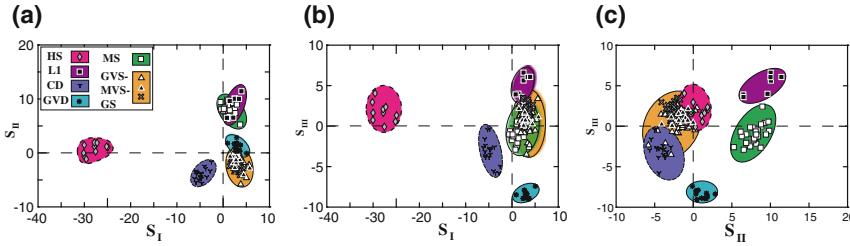


Fig. 3 Principal Component diagrams obtained from the FS-DFA method applied to the GVSC after Galerne et al. (2008). **a**, **b** and **c** show the best results for the sample populations used as input data. The applications of these

discriminant functions on samples from localities with too few samples to use statistics gave additional details on the GVSC geochemical architecture (see Fig. 10 d–f in Galerne et al. 2008)

analysis to predict a categorical dependent variable (called a *grouping variable*) on the basis of a set of independent variables (called *predictor variables*). Discriminant analysis is used when groups are known a priori (unlike in cluster analysis). It works by creating one or more linear combinations of predictors, called *discriminant functions* (or *principal component functions*). The number of discriminant functions possible is either $n - 1$ ($n =$ number of groups), or p (the number of predictors), whichever is smaller. The first function created maximizes the differences between groups on that function. The second function maximizes differences on that function, but also must not be correlated with the previous function. This continues with subsequent functions with the requirement that the new function is not correlated with any of the previous functions.

In geological fingerprinting by the FS-DFA method, n is a set of known sample populations or groups (i.e. lavas, dykes, sills); the predictor variables, p , are chemical variables within each population (major elements, trace elements, isotope ratios). The higher p , the more detailed and reliable are the results. Using such input information the FS-DFA evaluates the compositional variations within each sample population, and the geochemical differences between the sample populations. The resulting basis functions are based on the most discriminative predictor variables, m ($< p$), weighted by the coefficients, W , that maximize the variance between the populations relative to the

variance within them. These weighted variables are combined in $n - 1$ basis functions (assuming that $n < m$). An example of such statistical analysis can be found in Table 3 in Galerne et al. (2008). The general formulation of the discriminant (or principal component) function is:

$$S_i = C_i + W_i^1 \cdot X_i^1 + W_i^2 \cdot X_i^2 + \dots + W_i^m \cdot X_i^m \quad (1)$$

where C is a constant specific to the i th discriminant function S ; X is the measured concentration of a given element, weighted by the coefficient W specific to that element X in the i th discriminant function. The subscript i refers to the relative importance of the discriminant functions, 1 giving the best discrimination, $n - 1$ the poorest; the superscripts 1 to m refer to the predictors (elements, isotope ratios) included in the final model. The statistical method has the advantage that it can deal with large data sets and produce quick and robust results (see Fig. 11 in Galerne et al. 2008).

The result may be presented in two-dimensional plots using the best discriminative functions as main axes (Fig. 3). It is also possible to show the populations in a hierarchical diagram which displays the relative compositional differences between the populations (Fig. 4). Below we show the use of the FS-DFA method on the Golden Valley Sill Complex in the Karoo Basin, South Africa.

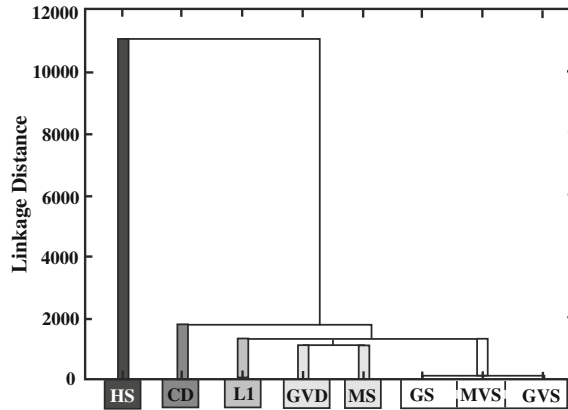


Fig. 4 Hierarchical diagram representing Single Linkage Euclidean distances between the eight main units in the GVSC (i.e. saucer-shaped sills, sills and dykes). The distance along the Y-axis shows the relative differences in chemistry between the centres of the populations. These values are computed using the “nearest neighbours” across the population groups (units) to determine the relative difference between them. The GS, MVS and GVS

groups show no compositional difference and are therefore attributed with a single linkage distance value close to 0. The chemically distinct HS group has the highest single linkage distance value. The different levels of relative chemical differences are reflected by the distinct branches of the hierarchical tree highlighted here with different grey scale colours. Figure modified after Galerne et al. (2008)

3 Application to the Golden Valley Sill Complex (GVSC), Karoo Basin, South Africa

Outside the Lesotho Lava Plateau, erosion has exposed a large number of sills and numerous dykes that represent the uppermost part of the plumbing system in the Karoo Large Igneous Province (LIP). Estimates suggest that sills in the Karoo Basin make up a total volume of 277,000 km³ (Svensen et al. 2014). The Golden Valley Sill Complex (GVSC) consist of large and small sills and dykes within a limited area (~850 km²) in the Karoo Basin. The area is representative of the Karoo Basin outside the Lesotho Plateau (Fig. 5a). Structural units (i.e. sills and dykes, each represented by a specific sample population), may be easily distinguished in a map view, but their genetic relationships are unknown. Few physical contacts exist between sills and dykes in the GVSC, thus numerous genetic relationships may be imagined: from (a) all units originate in the same, or identical, magma batches, to (b) all units are derived from

separate magma batches (Galerie et al. 2008, 2010). The genetic relationship has important bearing on our understanding of the intrusion mechanisms and feeding systematics of sill complexes.

The Karoo LIP was emplaced between 184 and 177 Ma (Encarnación et al. 1996; Le Gall et al. 2002; Jourdan et al. 2004, 2005, 2007; Svensen et al. 2012) with a peak of activity at 183 Ma, corresponding to the main period of emplacement of the Karoo sills and dykes (Svensen et al. 2012). The GVSC is located in the southern part of the Karoo Basin, SW of the Lesotho Lava Plateau, and consists of four major elliptical saucer-shaped sills and a major dyke (Fig. 5a; Galerie et al. 2008). The GVSC area also includes the Golden Valley Dyke (GVD; ≤15 m thick, 17 km long) and several small dykes (d1–d4) and short sill segments (e.g., L1, L2 and L3). The large sills are emplaced in two stratigraphic levels: the Morning Sun Sill (MSS) and the Harmony Sill (HS) at the deeper level, and the Golden Valley Sill (GVS) and the Glen Sill (GS) at a slightly higher level. Each sill at the higher level is located above a sill at the lower level.

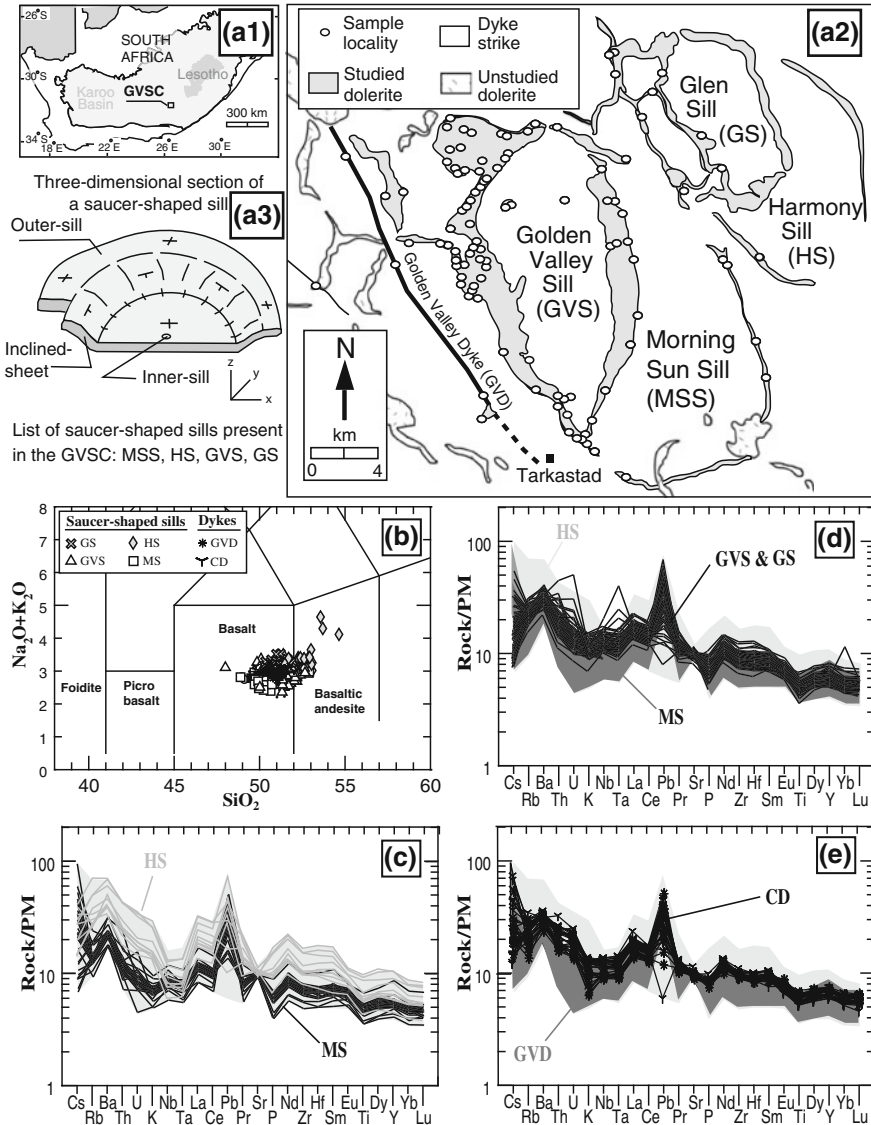


Fig. 5 **a1** Location of the GVSC in the Karoo Basin, South Africa. **a2** Simplified geological map of the GVSC showing sample locations (after Galerne et al. 2008). **a3** Schematic illustration of saucer-shaped sill in three-dimensional cross-section. **b** Total Alkali Silica (TAS)

diagram **c–e** Trace element concentrations (normalized to Primitive mantle, PM, as given by McDonough and Sun 1995) for rocks in the golden valley Sill Complex (Galerie et al. 2008)

All the rocks in the GVSC are basaltic to basaltic-andesitic (Fig. 5b) and the compositional range is generally small (Fig. 5b–e). The samples show essentially parallel trace-element patterns which might be explained by different degrees of fractional crystallization from a common initial magma. The southern part of the Karoo Basin is

underlain by the Namaqua-Natal Mobile Belt in which the lithosphere acquired an arc-like signature (enriched Sr–Nd isotope ratios, negative Nb–Ta anomalies) during former orogenic events (e.g., Catuneanu 2004); Strong enrichment in Pb indicates crustal contamination (Fig. 5d–e). However, plots of ratios between pairs of incompatible

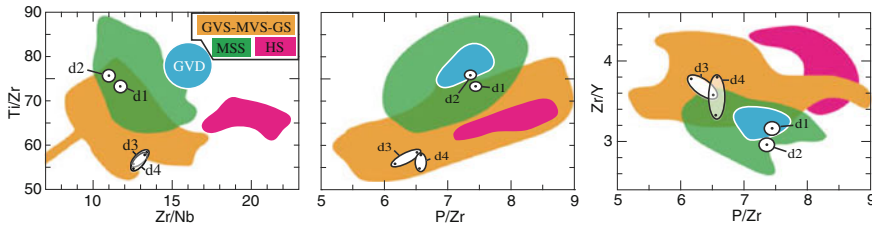


Fig. 6 Plots of strongly incompatible element ratios (Ti/Zr vs. Zr/Nb, Ti/Zr vs. P/Zr, and Zr/Y vs. P/Zr) in dolerites from the GVSC (modified after Galerne et al. 2008, 2011). Data published in Fig. 15 of Galerne et al.

(2008) are completed with the data published as supplementary material by Galerne et al. (2008). The colored fields represent the distinct magma batches involved in the emplacement of major sills and dykes of the GVSC

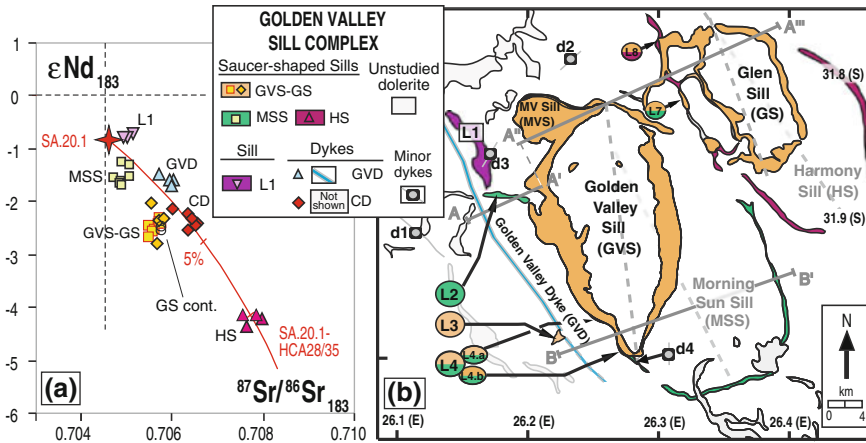


Fig. 7 a Variations in initial Sr–Nd isotopes among the GVSC units (after Neumann et al. 2011), assuming the age of 183 Ma determined for sills in the Karoo Basin (Svensen et al. 2007, 2012). The trend is estimated on the basis of the EC-RAFC model of Spera and Bohrsen (2004) using dyke SA.20.1 from southern KwaZulu-Natal, South Africa (Riley et al. 2006) as initial-melt

model and a combination of the Proterozoic mafic granulite xenoliths HCA28 and HCA35 from the northern Lesotho/central Cape province (Huang et al. 1995). **b** Map view of the Geochemical architecture of the GVSC (Galerie et al. 2008). Different colors reflect different chemical signatures

elements (Fig. 6) show clear distinctions between some of the populations. It is particularly evident that the geochemical characteristics of the HS and the GVD are different from those of the other units. However, the FS-DFA statistical method, based on 47 major and trace elements, reduced to 19 most discriminative predictor variables (*m*) by the PCA algorithm, gives an excellent separation of the populations (Fig. 3). Although some populations overlap in some diagrams, they are separated in others, showing that the units, or sample populations, are separated in *m*-dimensional space. The results are presented in map view in Fig. 7b. The

degree of chemical diversity among the populations is shown in the hierarchical diagram, Fig. 4. Two units, the Golden Valley Sill (GVS) and the Glen Sill (GS) overlap in all diagrams, and are shown as identical in the hierarchal diagram, the other units have different chemical fingerprinting. This means that GVS and GS must originate in the same, or identical, magma batches, whereas the other populations in the GVSC were derived from separate magma batches.

The FS-DFA method also helped in the study of the GVSC regarding some units for which there were too few analyses to give a statistical

basis. Once the basis functions were established, it was possible to estimate the positions of samples from these units in the Principal Component diagrams and thus test their possible affinity to the other units (and magma batches; see Fig. 10 in Galerne et al. 2008). This increased the details of known genetic relationships in the GVSC. The overall result is the comprehensive geochemical architecture shown in map view in Fig. 7b.

In the GVSC the results obtained by the FS-DFA method were later confirmed by Sr–Nd isotope data (Fig. 7a; Neumann et al. 2011). Each unit that was given a unique geochemical identity by the FS-DFA method based on major and trace element data, covered a very limited range in $^{87}\text{Sr}/^{86}\text{Sr}$ and $^{143}\text{Nd}/^{144}\text{Nd}$ ratios, defining a small domain different from those of the other units. Furthermore, like in the Principal Component diagram (Fig. 3), the GVS and GS showed identical Sr–Nd isotope ratios, confirming derivation from the same (or identical) magma batches.

4 Implications

4.1 Genetic Relationship and Evolutionary History

Geochemical fingerprinting can reveal details about the genetic relationships between magmatic rocks in an area, and about their evolutionary history. Based on major and trace element and Sr–Nd isotope data Neumann et al. (2011) concluded that the different geochemical signatures in the different units in the Golden Valley Sill Complex were caused by a combination of interaction with the lithospheric mantle and fractional crystallization and contamination in the deep crust. The ascending magmas lost their buoyancy when passing from the dense upper mantle into the less dense lower crust, and ponded there. The hot magmas heated the crustal wall-rocks beyond their solidus temperatures, causing partial melting. At the same time the magmas cooled and started to crystallize. Different degrees of hybridism of crustal melts with strong arc-type geochemical signature,

accompanied by fractional crystallization (AFC processes) changed the major and trace element, and the Sr–Nd isotope compositions of the magmas, thus causing their different geochemical fingerprinting (Figs. 6 and 7). Hybridism of lower crustal melts led to different degrees of enrichment in strongly incompatible elements, enriched Sr–Nd isotopic ratios, and relative depletion in Nb and Ta relative to REE. In summary the different magmas appear to be derived from a common, or identical, primary melt(s). Entering the lower crust the melt(s) formed magma chambers where they were subjected to different degrees of fractional crystallization and contamination. This gave rise to magma batches with different chemical fingerprinting which have given very important information about the feeding mechanisms and plumbing system in the upper crust.

4.2 Emplacement Mechanism of the GVSC Plumbing System

Saucer-shaped sills are tabular intrusions observed worldwide in volcanic margins and sedimentary basins (e.g., offshore Norway, Karoo Basin). Although they are common, their feeding mechanisms are poorly known, mainly because the relationships between sills and their feeders are rarely exposed (e.g., Hyndman and Alt 1987), and difficult to image on seismic data. The emplacement mechanism of sills and saucer-shaped sills in sedimentary basins are therefore mostly debated on the basis of theoretical models. Some models propose that sill intrusions occur along the level of neutral buoyancy of the magma, and the feeders are expected to be located below the outer sill at one side of the saucer (Fig. 8a; e.g., Bradley 1965; Francis 1982; Chevallier and Woodford 1999; Gouly 2005); other models propose that saucers are fed from below through a central feeder dyke (Fig. 8b; Galland et al. 2009, and references therein). In the latter models, the feeders are expected to be situated beneath the central part of the inner sills (Fig. 8b).

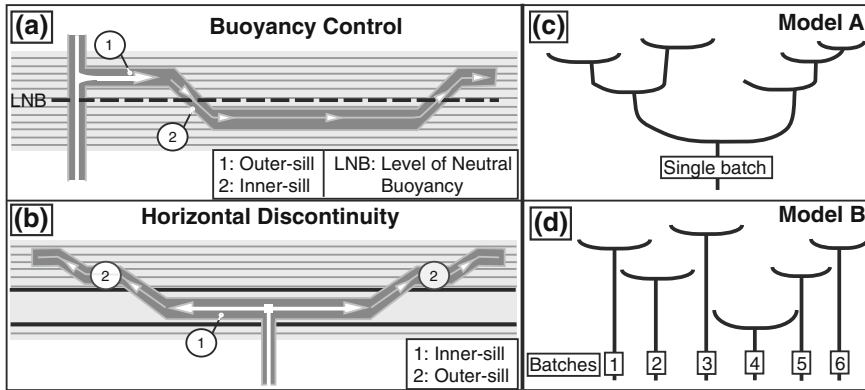


Fig. 8 **a** and **b** are theoretical models of saucer-shaped sill emplacement mechanisms. Numbers (1) and (2) indicate the steps of emplacement. **a**. Model of emplacement controlled at the level of neutral buoyancy (LNB), modified from Francis (1982). Sills are fed laterally from one part of the outer sill. **b** Model of emplacement along horizontal discontinuity, modified after Malthe-Sørenssen

et al. (2004). Sills are fed radially from the inner sill. **c** and **d** are geochemical end-member plumbing system scenarios for sill complexes. **c** Model A: a single batch of magma forms a network of interconnected (nested) sills. **d** Model B: each saucer-shaped sill represents a geochemical distinct magma batch that has entered the upper crust through separate channels

The application of the geochemical fingerprinting method to saucer-shaped sill complexes may help deciphering which of these theoretical models works in nature. The problem is reformulated as follows: are the sills in saucer-shaped sill complexes formed by a single magma batch through an interconnected network (Model A; Fig. 8c), or is each unit in such a complex fed by an individual magma batch (Model B; Fig. 8d)? The first hypothesis implies that the sills fed each other through an interconnected sill network (Fig. 8c); the second hypothesis implies that each sill is fed through a distinct conduit (Fig. 8d).

In the GVSC a small part of the vertical section is exposed, revealing part of the 3-D relationship between sills and dykes. Combined with field relationships, structural observations and mechanical considerations, the application of chemical fingerprinting provides an important tool to establish the architecture of the upper parts of plumbing systems and the feeding relationship between different units.

As shown above, the FS-DFA statistical method revealed that in the GVSC the two major saucers at the upper stratigraphic level (GVS and GS) have identical chemical fingerprinting (Figs. 4 and 5). This indicates that, although they are not presently in physical contact, they

originate from the same, or identical, magma batches. All other major intrusions yield distinctive geochemical signatures. This implies that the sills at the upper (GVS and GS) and lower levels (HS and MSS) were not connected in a sill-feeding-sill relationship while emplaced in the Karoo Basin (Fig. 9a, b).

Some minor sills are in physical contact with major sills or dykes (L3-GVD, L4-GVS, L7-GS and L8-GS; Fig. 7b), suggesting sill-feeding-sill relationships. However, the FS-DFA results show that L4, L7 and L8 consist of two parts, an upper part with GVS-GS geochemical signature and a lower part with MSS signature (Galerie et al. 2008). These locations reveal that the MSS at the lower stratigraphic level locally came into contact with the GVS-GS at the higher stratigraphic level, but there is no sill-feeding-sill relationship (Figs. 8 and 9).

There are, however, close associations between one elliptical sill (the GVS) and a small dyke (d4): the dyke is exposed underneath the southern tip of the sill, and is parallel to the long axis of the GVS sill (dashed line in Fig. 7b). Unfortunately only two analyses with significantly fewer trace elements than in the main data set were available on d4. To determine their geochemical relationship the GVS and dyke d4

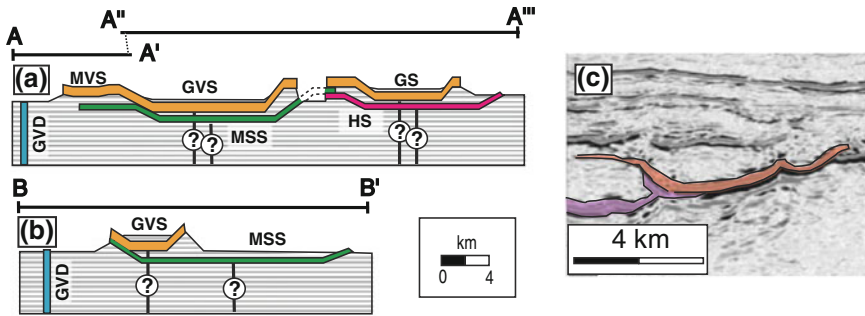


Fig. 9 Geological cross-sections **a** A-A''' and **b** B-B'. Figure after Galerne et al. (2011), see Fig. 6 for colour legend. **c** Example of seismic image showing contact between two saucer-shaped sills, interpreted as feeding relationship by Hansen et al. (2004). A comparison

between this image and the geological cross section of the GVSC suggests that the contact between the two sills may not reflect a feeding relationship, but is accidental, as suggested by the different colors in this hypothetical re-interpretation

data were compared on the basis of element ratios (Fig. 6). In all diagrams d4 falls within the field defined by the GVS-GS magma batch. Having the same geochemical signature as the GVS, the d4 dyke covers all fundamental criteria required for being the feeder of the overlying saucer-shaped GVS sill: it is stratigraphically below the GVS, aligned along the long axis of the sill, and has identical geochemical signatures.

The above discussion shows that the plumbing system in the GVSC closely resembles Model B in Fig. 9d with each unit being fed by a separate batch of magma (Galerne et al. 2008, 2011). However, their identical geochemical signatures leave the possibility that GVS fed GS through a lateral overflow and that a former contact between the two sills has been erased by erosion (Galerne et al. 2008). This possibility was, however, made unlikely by laboratory experiments combined with recent field work in the GVSC (Galerne et al. 2011). Experiments on the relationships between type of feeder (one-dimensional or dyke) and the shape of saucer-shaped sills suggest that the most likely feeder to an elliptical saucer-shaped sill is a dyke located underneath the sill, oriented parallel to the long axis of the elliptical sill (Galerne et al. 2011). The experimental results show strong similarities to the GVS-d4 relationships and thus support the proposition that dyke d4 is the feeder to the GVS sill (Galerne et al. 2011). Also the other saucer-shaped sills in the GVSC are elliptical. Based on

these experiments it seems likely that all the GVSC sills are fed by separate dykes. Despite identical geochemical signatures of the GVS and GS, these two sills may also have had separate feeder dykes in the upper crust.

The experimental technique and apparatus used in the laboratory experiments that gave rise to the dyke-feeding-elliptical-sill hypothesis were developed by Galland et al. (2009). Details on this method may be found in “Laboratory experiments” in the present volume (Galland et al. 2014). This is important information also when it comes to interpreting saucer-shaped sills that appear to be nested in images based on seismic data (Fig. 9c). Saucer-shaped sills showing contact in seismic images are generally interpreted in terms of sill-feeding-sill (Hansen et al. 2004). However, the results from the GVSC strongly suggest that such contacts may be accidental, and have no bearing on the genetic relationship between the sills. The alternative interpretation of two sills in contact but genetically unrelated are suggested in Fig. 9c.

5 Summary and Perspectives

Chemical fingerprinting is an old method in geochemistry. Since the work of Pearce and Cann (1971, 1973) this method has kept evolving as the resolution of chemical analyses increase. Technical improvements have brought geochemical

fingerprinting into a new era where it can be used to distinguish magmatic units emplaced or erupted in restricted areas within a given tectonic setting on the basis of subtle geochemical contrasts.

Theoretical models based on mechanistic approaches and/or observations often result in numerous competing models. Geochemical fingerprinting provides a tool to identify the geochemical architecture of magmatic systems. This technique appears to be a robust method to support or reject theoretical models. We have provided two examples of successful application of the geochemical fingerprinting method to flood basalts and a sill complex emplaced in sedimentary basin. In the case of the flood basalts, the results provided the possibility of correlating lavas in stratigraphic sections that are separated by erosion and spread over distances of 100s of km. The results gave information on time-related compositional variations on the same scale, and confirmed the large extent of surface eruptions of the same magma batch, either through continuous connection or separate co-eruptive fissures. In the case of sill complex emplacements in a sedimentary basin, geochemical fingerprinting showed that a large complex of apparently interconnected sills (saucer-shaped sills) were not feeding one another but formed from separate magma batches, and that one of the major sills was fed by a dyke.

References

- Bradley J (1965) Intrusion of major dolerite sills. *Trans R Soc NZ* 3:27–55
- Catuneanu O (2004) Retroarc foreland systems—evolution through time. *J Afr Earth Sc* 38(3):225–242
- Chevallier L, Woodford A (1999) Morpho-tectonics and mechanism of emplacement of the dolerite rings and sills of the western Karoo, South Africa. *S Afr J Geol* 102(1):43–54
- Duncan AR, Erlank AJ, Marsh JS (1984) Regional geochemistry of the Karoo igneous province. In: Erlank AJ (ed) *Petrogenesis of the volcanic rocks of the Karoo province*. *Geol Soc of S Afr Spl Pub*, pp 355–388
- Encarnación J, Fleming TH, Eales HV (1996) Synchronous emplacement of Ferrar and Karoo dolerites and the early breakup of Gondwana. *Geology* 24:535–538
- Francis EH (1982) Magma and sediment—I. Emplacement mechanism of late Carboniferous tholeiite sills in northern Britain. *J Geol Soc* 139(1):1–20
- Galerne CY, Neumann ER, Planke S (2008) Emplacement mechanisms of sill complexes: information from the geochemical architecture of the golden valley sill complex South Africa. *J Volcanol Geoth Res* 177(2):425–440
- Galerne CY, Neumann ER, Aarnes I, Planke S (2010) Magmatic differentiation processes in saucer-shaped sills: Evidence from the golden valley sill in the Karoo Basin, South Africa. *Geosphere* 6(3):163–188
- Galerne CY, Galland O, Neumann ER, Planke S (2011) 3D relationships between sills and their feeders: evidence from the golden valley sill complex (Karoo Basin) and experimental modelling. *J Volcanol Geoth Res* 202(3–4):189–199
- Galland O, Holohan E, van Wyk de Vries B, Burchardt S (2014) Laboratory modelling of volcano plumbing system. In: Breitreuz C, Rocchi S (eds) *Laccoliths, sills and dykes—physical geology of shallow level magmatic systems*. *Advances in volcanology*
- Galland O, Planke S, Neumann ER, Malthe-Sørenssen A (2009) Experimental modelling of shallow magma emplacement: application to saucer-shaped intrusions. *Earth Planet Sci Lett* 277(3–4):373–383
- Gouly NR (2005) Emplacement mechanism of the Great Whin and Midland Valley dolerite sills. *J Geol Soc* 162:1047–1056
- Hansen DM, Cartwright JA, Thomas D (2004) 3D seismic analysis of the geometry of igneous sills and sill junctions relationships. In: Davies RJ, Cartwright JA, Stewart SA, Lappin M, Underhill JR (eds) *3D Seismic technology: application to the exploration of sedimentary basins*. Geological Society, London, *Memoirs* pp 199–208
- Hill T, Lewicki P (2007) *STATISTICS: methods and applications*. StatSoft, Tulsa
- Huang Y, van Calsteren P, Hawkesworth C (1995) The evolution of the lithosphere in southern Africa: A perspective on the basic granulite xenoliths from kimberlites in South Africa. *Geochim Cosmochim Acta* 59(23):4905–4920
- Hyndman DW, Alt D (1987) Radial dikes, laccoliths, and gelatin models. *J Geol* 95:763–774
- Jourdan F, Feraud G, Bertrand H, Kampunzu AB, Tshoso G, Le Gall B, Tiercelin JJ, Capiez P (2004) The Karoo triple junction questioned: evidence from Jurassic and Proterozoic Ar-40/Ar-39 ages and geochemistry of the giant Okavango dyke swarm (Botswana). *Earth Planet Sci Lett* 222(3–4):989–1006
- Jourdan F, Feraud G, Bertrand H, Kampunzu AB, Tshoso G, Watkeys MK, Le Gall B (2005) Karoo large igneous province: Brevity, origin, and relation to mass extinction questioned by new Ar-40/Ar-39 age data. *Geology* 33(9):745–748
- Jourdan F, Feraud G, Bertrand H, Watkeys MK (2007) From flood basalts to the inception of oceanization: Example from the Ar-40/Ar-39 high-resolution picture

- of the Karoo large igneous province. *Geochem Geophys Geosyst* 8(2):1–20
- Le Gall B, Tshoso G, Jourdan F, Feraud G, Bertrand H, Tiercelin JJ, Kampunzu AB, Modisi MP, Dymont J, Maia M (2002) Ar-40/Ar-39 geochronology and structural data from the giant Okavango and related mafic dyke swarms, Karoo igneous province, northern Botswana. *Earth Planet Sci Lett* 202(3–4):595–606
- Malthe-Sørenssen A, Planke S, Svensen H, Jamtveit B (2004) Formation of saucer-shaped sills. In: Breikreuz C, Petford N (eds) *Physical geology of high-level magmatic systems*. Geological Society, London, *Spl Pub* pp 215–227
- Marsh JS, Hooper PR, Rehacek J, Duncan RA, Duncan AR (1997) Stratigraphy and age of Karoo basalts of Lesotho and implications for correlations within the Karoo igneous province. In: Mahoney JJ, Coffin MF (eds) *Large igneous provinces: continental, oceanic, and planetary flood volcanism*. Geophysical Monographs Series. American Geophysical Union, pp 247–272
- McDonough WF, Sun SS (1995) The composition of the earth. *Chem Geol* 120(3–4):223–253
- Neumann ER, Svensen H, Galerne CY, Planke S (2011) Multistage evolution of dolerites in the Karoo Large Igneous Province, Central South Africa. *J Petrol* 52(5):959–984
- Pearce J, Cann J (1971) Ophiolite origin investigated by discriminant analysis using Ti, Zr and Y. *Earth Planet Sci Lett* 12(3):339–349
- Pearce J, Cann J (1973) Tectonic setting of basic volcanic-rocks determined using trace-element analyses. *Earth Planet Sci Lett* 19(2):290–300
- Riley TR, Curtis ML, Leat PT, Watkeys MK, Duncan RA, Millar IL, Owens WH (2006) Overlap of Karoo and Ferrar magma types in KwaZulu-Natal, South Africa. *J Petrol* 47(3):541–566
- Sheth HC, Mahoney JJ, Chandrasekharam D (2004) Geochemical stratigraphy of Deccan flood basalts of the Bijasan Ghat section, Satpura Range, India. *J Asian Earth Sci* 23(1):127–139
- Spera F, Bohron W (2004) Open-system magma chamber evolution: an energy-constrained geochemical model incorporating the effects of concurrent eruption, recharge, variable assimilation and fractional crystallization (EC-E RA chi FC). *J Petrol* 45(12):2459–2480
- StatSoft Inc (2013) *Electronic statistics textbook*. Tulsa, OK. <http://www.statsoft.com/textbook/>
- Svensen H, Corfu F, Polteau S, Hammer O, Planke S (2012) Rapid magma emplacement in the Karoo Large Igneous Province. *Earth Planet Sci Lett* 325:1–9
- Svensen H, Planke S, Chevallier L, Malthe-Sørenssen A, Corfu F, Jamtveit B (2007) Hydrothermal venting of greenhouse gases triggering early Jurassic global warming. *Earth Planet Sci Lett* 256(3–4):554–566
- Svensen H, Polteau S, Cawthorn S, Planke S (2014) Subvolcanic intrusions in the Karoo Basin, South Africa. In: Breikreuz C, Rocchi S (eds) *Laccoliths, sills and dykes—physical geology of shallow magmatic systems*. *Advances in Volcanology*